DR

CONF-780783--1

MASTER

PRESENTED AT

American Association of Physicists in Medicine
Twentieth Annual Meeting
San Francisco, California
July 30 - August 3, 1978

ANALYSIS OF FACTORS LIMITING THE GEOMETRIC RESOLUTION OF A POSITRON IMAGING DEVICE

Frank B. Atkins, Paul V. Harper, and Robert N. Beck

Department of Radiology of The University of Chicago
and The Franklin McLean Memorial Research Institute*
Chicago, Illinois 60637

* Operated by The University of Chicago for the U.S. Department of Energy under Contract No. EY-76-C-02-0069.

There has been continuing interest over the past several years in the application of positron-emitting radiopharmaceuticals to studies of metabolic function in-vivo. With these investigations as the objective, there have been many new developments in positron imaging systems. In particular, systems which use large-area, position-sensitive elements as the detectors, have been used successfully.

These devices are not limited in spatial resolution by mechanical collimation as is the case for conventional imaging systems. The necessary directional information is obtained from the simultaneous detection of the annihilation photon pair and the assumption of colinearity of their trajectories. There are, however, a number of factors which place limitations on the achievable geometric resolution. Some of these are dependent upon the detector system employed, while a few are intrinsic to the positron emission and annihilation processes. This latter type represents a fundamental limit in system resolution. Those properties which ~~which~~ will be discussed are shown in the first slide.

SLIDE 1

These include the intrinsic spatial resolution of the detector, parallax errors due to an oblique incidence of the annihilation photons on detectors of finite thickness, the range of the emitted positrons in tissue before they annihilate, and the angular deviation of the coincident photons from 180°.

SLIDE 1

COMPONENTS AFFECTING THE SPATIAL RESOLUTION OF AN ANNIHILATION COINCIDENCE SYSTEM
1. Intrinsic spatial resolution of the detector 2. Parallax errors due to the oblique incidence of photons on a detector of finite thickness 3. Range of the emitted positron in tissue 4. Angular deviation of the coincident photon pair from colinearity

An experimental investigation of these components is difficult simply because they often cannot be isolated from one another. Thus we have chosen a Monte Carlo approach for this analysis. These computer simulations permit a detailed investigation of the effects of these various factors on the system resolution; both individually, as well as collectively.

The subsequent discussions of system resolution are defined in terms of the point or line source image obtained by back projecting the rays defined by the apparent coordinates of the two coincident photons in each detector through the plane containing the source.

SLIDE 2

The limited spatial resolution inherent in all position-sensitive detector systems, in most cases, represents the greatest loss in image quality. For a system employing scintillation cameras, the intrinsic resolution might have a FWHM of 6-8 mm at 511 keV.

The back-projected image, as shown on the left, is given by the density of intersections of the rays which define the apparent end points of the coincident event in the two detectors. If (ξ_1,η_1) and (ξ_2,η_2) are these X and Y coordinates, then the point of intersection is simply given by this set of linear equations on the right. In this case Z is the displacement of the source from the midline, and S is the detector separation. Since the

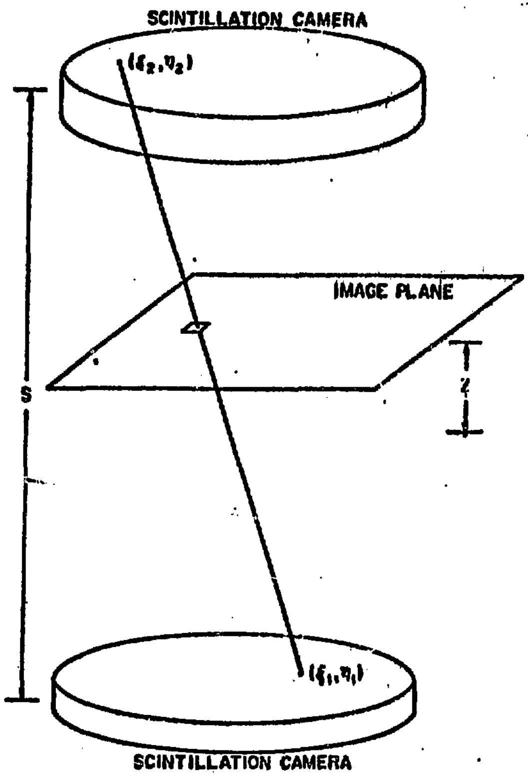

FORMATION OF THE BACK-PROJECTION IMAGE USING COINCIDENCE DETECTION

If (ξ_1, η_1) and (ξ_2, η_2) are the coordinates of the event in the two detectors, then the ray joining these points intercepts the image plane at:

$$x = \alpha\xi_1 + \beta\xi_2$$

$$y = \alpha\eta_1 + \beta\eta_2$$

where

$$\alpha = \left(\frac{1}{2} - \frac{Z}{S}\right)$$

$$\beta = \left(\frac{1}{2} + \frac{Z}{S}\right)$$

detection of the two annihilation photons are independent processes, we can consider these equations as the sum of two random variables. In the next slide we can write the expressions for the coincident point source response function.

SLIDE 3

In this expression, P represents the probability that a particular coordinate will be observed. In order for the ray to pass through the point (x,y), then ξ_2 and η_2 must satisfy the expressions shown obtained from the equations on the previous slide. Changing the variable of integration, this reduces to the bottom equation.

As an example, we can consider a scintillation camera which has an intrinsic spatial resolution which is approximately Gaussian in form. Assuming identical characteristics for both detectors, then this convolution equation becomes separable.

SLIDE 4

If σ is the intrinsic resolution factor, then it can be shown that in the coincidence mode the response function is likewise Gaussian with a variance given by the expression shown. The factors β and γ are functions of the displacement of the source from the midplane. This factor has its minimum value at the center, where the resolution is improved by a factor of $\sqrt{2}$ over the intrinsic resolution. At the other extreme, where the source is at the detector, the resolution approaches σ.

SLIDE 3

The coincident point source response function due to the intrinsic detector spatial resolution is given by

$$psrf(x,y) = \iint P(\xi_1,\eta_1)P\left(\frac{x - \alpha\xi_1}{\beta}, \frac{y - \alpha\eta_1}{\beta}\right)d\xi_1 d\eta_1 \quad .$$

Following a change in variables this becomes

$$psrf(\beta x',\beta y') = \iint P(\xi_1,\eta_1)P(x' - \gamma\xi_1, y' - \gamma\eta_1)d\xi_1 d\eta_1$$

where $\gamma = \alpha/\beta$

SLIDE 4

EVALUATION FOR A GAUSSIAN DETECTOR RESPONSE FUNCTION

If σ is the resolution factor of the detectors in a non-coincident mode, then it can be shown that:

1. the response function for the coincidence mode is also a Gaussian

2. the resolution factor is given by

$$\sigma_c = \beta\sigma\sqrt{1 + \gamma^2}$$

A simulation of this component was performed in the following manner. Assume that the source is located in the midplane. An initial direction of emission of the annihilation photons was chosen at random from an isotropic distribution. This was accomplished by sampling uniformly from the surface of a sphere. The coordinates of this ray were then determined in the two detector planes. A Gaussian distributed random variable with zero mean was then added to the X and Y coordinates of each detector.

SLIDE 5

The simulated data were then back-projected to yield the response function shown by the histogram plot. The solid line is the corresponding theoretical expected response function based on the preceding analysis, and there is very good agreement between the two.

The second factor to consider is due to the oblique incidence of the photons on the detector.

SLIDE 6

In order for any imaging system to have a reasonable detection efficiency for the 511 keV photons, the detectors must have a finite thickness. Coincidence detection permits valid events in which the photons are incident on the detectors at relatively steep angles as shown by the ray in this figure. The maximum angle depends upon the detector size and separation, but typically this can

EFFECT OF DETECTOR RESOLUTION ON COINCIDENT RESPONSE FUNCTION

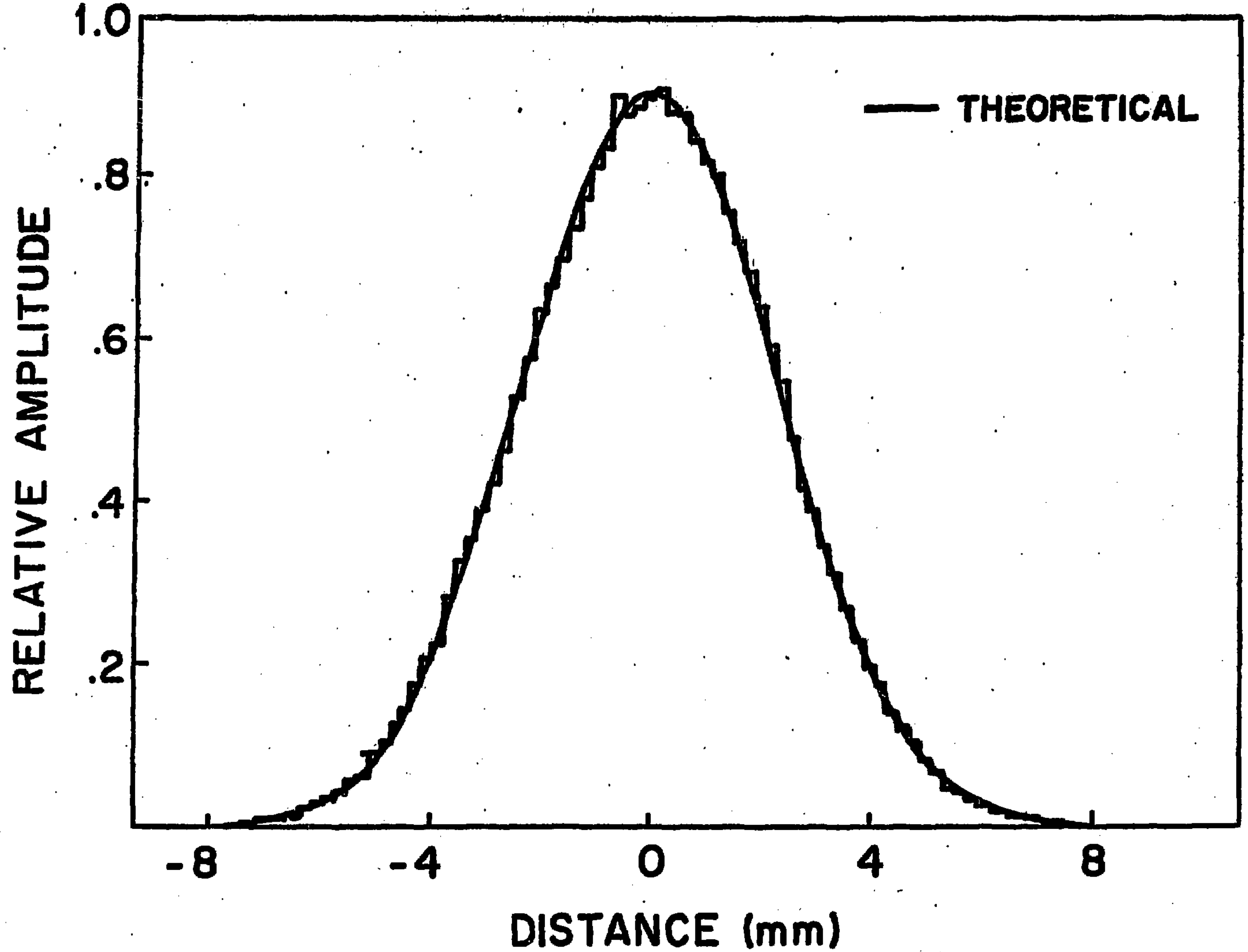

range to about 25-30°. The photon interaction, however, can occur at any depth within the crystal. Since this depth cannot normally be determined, there is an ambiguity in the coordinates of the true position of the event. This uncertainty increases with both increasing angle and detector thickness. The shaded area indicates one possible plane which passes through the source. Within this plane, photons are emitted at some angle θ as indicated. The path of these photons passes obliquely through the detectors. If we assume an exponential absorption of the photon within the crystal, then the shaded region at the upper surface of the detector indicates the probability density that the interaction occurs within that projected linear segment. The curve shown near the center represents the probability distribution of the back-projected rays summed over all angles within this plane.

It is possible to derive an expression for the coincident point spread function due to oblique incidence alone. This is outlined in the next slide.

SLIDE 7

The probability that a photon interaction occurs along an element of path length through the detector is exponential. This can be converted into a projected radial distance at the surface of the detectors. In the upper expression, r' is the radial coordinate in the image plane which contains the source. Since the interactions of the two annihilation photons are independent

SLIDE 6

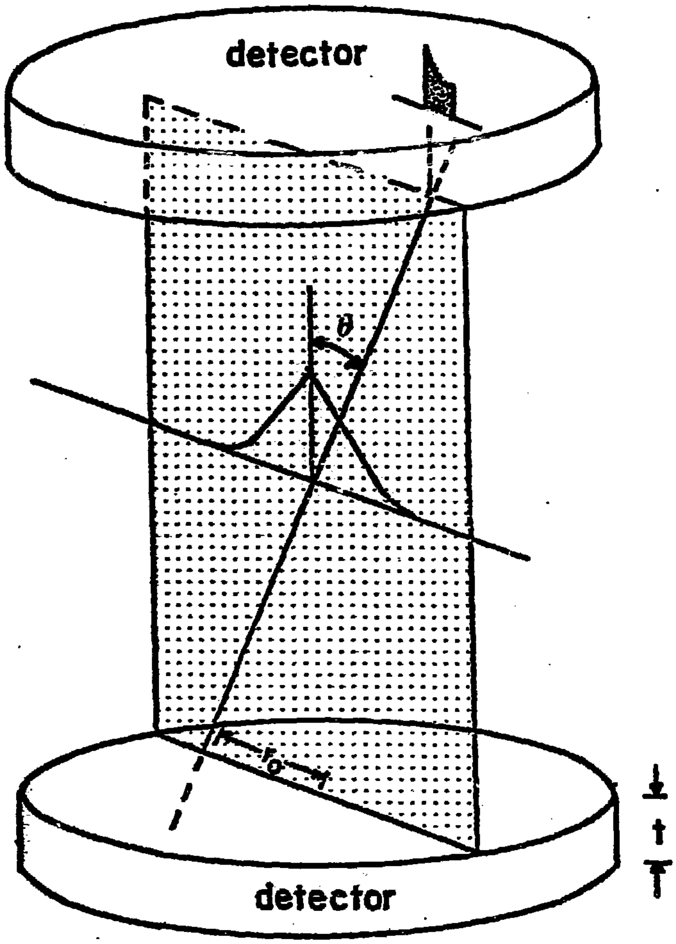

EFFECT OF THE OBLIQUE INCIDENCE ON THE COINCIDENT psf

COINCIDENT RESPONSE FUNCTION DUE TO OBLIQUE INCIDENCE

The probability that a photon interaction occurs along an element of path length is assumed to be exponential.

Let r' be the radial coordinate in the image plane which contains the source. The density function of the intersections is proportional to

$$f_{r'}(r') \propto \int_0^{\Delta r - 2r'} e^{-\mu\xi/\sin\theta} e^{-\mu(2r'+\xi)/\sin\theta} d\xi$$

Following integration this becomes

$$f_{r'}(r') \propto \left[e^{-2\mu r'/\sin\theta} - e^{-2\mu(\Delta r - r')/\sin\theta}\right]$$

The coincidence point source response function for oblique incidence is related to the density function by

$$\text{psrf}(r') \propto \frac{f_{r'}(r')}{2\pi r'}$$

processes, it can be shown that the probability density function of the random variable r' is proportional to this integral. Following the integration, we obtain the middle equation. This yields the triangular-shaped function that was plotted in the previous slide. The coincident response function is related to this density function by 1/r'.

This analysis was compared with the results of the simulations.

SLIDE 8

In this figure we have plotted the density function shown in the previous slide normalized to the value at zero distance. A detector thickness of 2.54 cm has been assumed. The Monte Carlo simulation of this component of the response assumed a simple exponential attenuation of the 511 keV photons passing through a NaI detector. The detector was assumed to have perfect spatial resolution, and that the centroid of the energy deposited within the detector by the photon corresponds to the point of interaction. In the simulations, mock photons are emitted isotropically from a source located in the midplane. Using the attenuation coefficient for the detector medium the distance to an interaction is selected at random for the two photons separately. If either interaction would occur outside the detector boundary, the event is discarded and a new one generated. If this results in a valid event, then the ray joining the end points is formed with the assumption that

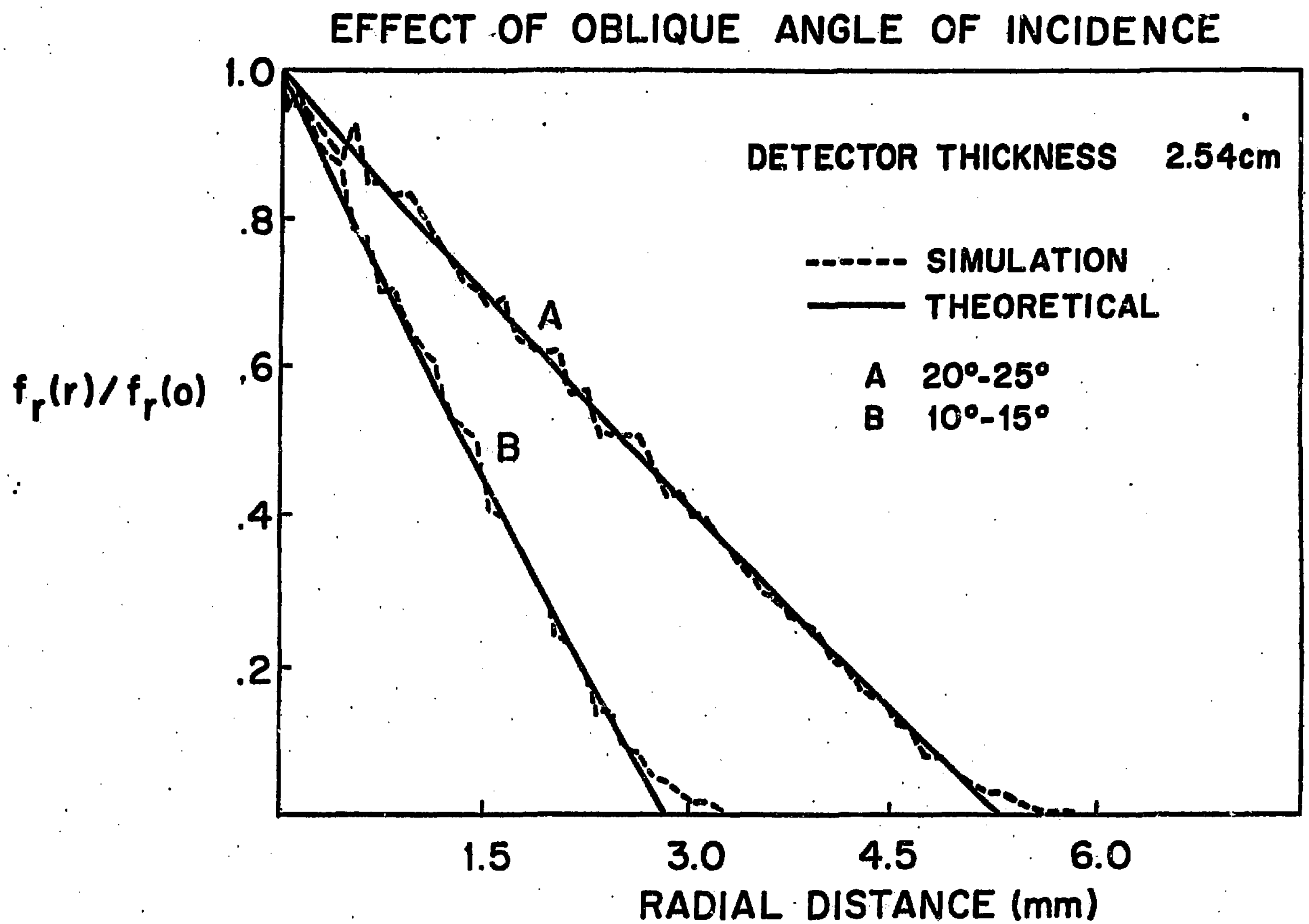
EFFECT OF OBLIQUE ANGLE OF INCIDENCE
DETECTOR THICKNESS 2.54cm
SIMULATION
THEORETICAL
A 20°-25°
B 10°-15°
A
B
1.0
.8
.6
.4
.2
$f_r(r)/f_r(o)$
1.5
3.0
4.5
6.0
RADIAL DISTANCE (mm)

the interaction took place at the detector surface. A few results are shown as the dashed curves in this figure for two angular ranges (10-15° and 20-25°). The solid curves are the theoretical values for an average incident angle within the two groups. The agreement between the theoretical and simulated data is seen to be quite good.

Coincident line spread functions due to this component are shown in the next slide.

SLIDE 9

The computed line spread functions for a 1"-thick NaI crystal are shown on the left and 1/2"-thick detector on the right. The upper curves are the response functions for a set of 5° angular intervals. The combined angular range, 0-25°, is shown at the bottom.

This results in a very peaked function because of the 1/r dependence in the point spread function. Even for a 1"-thick detector, this is seen to be a relatively narrow function.

One of the factors which is intrinsic to the process of positron emission and annihilation is the range over which the positron travels while losing kinetic energy until it is moving sufficiently slow to combine with an electron. This depends on the energy spectrum of the emitted positron. Consequently, this component of the image degradation is a function of the radionuclide under investigation. The nuclides chosen for the simulations are listed in the next slide along with some relevant characteristics.

COINCIDENT LSF DUE TO OBLIQUE ANGLE OF INCIDENCE

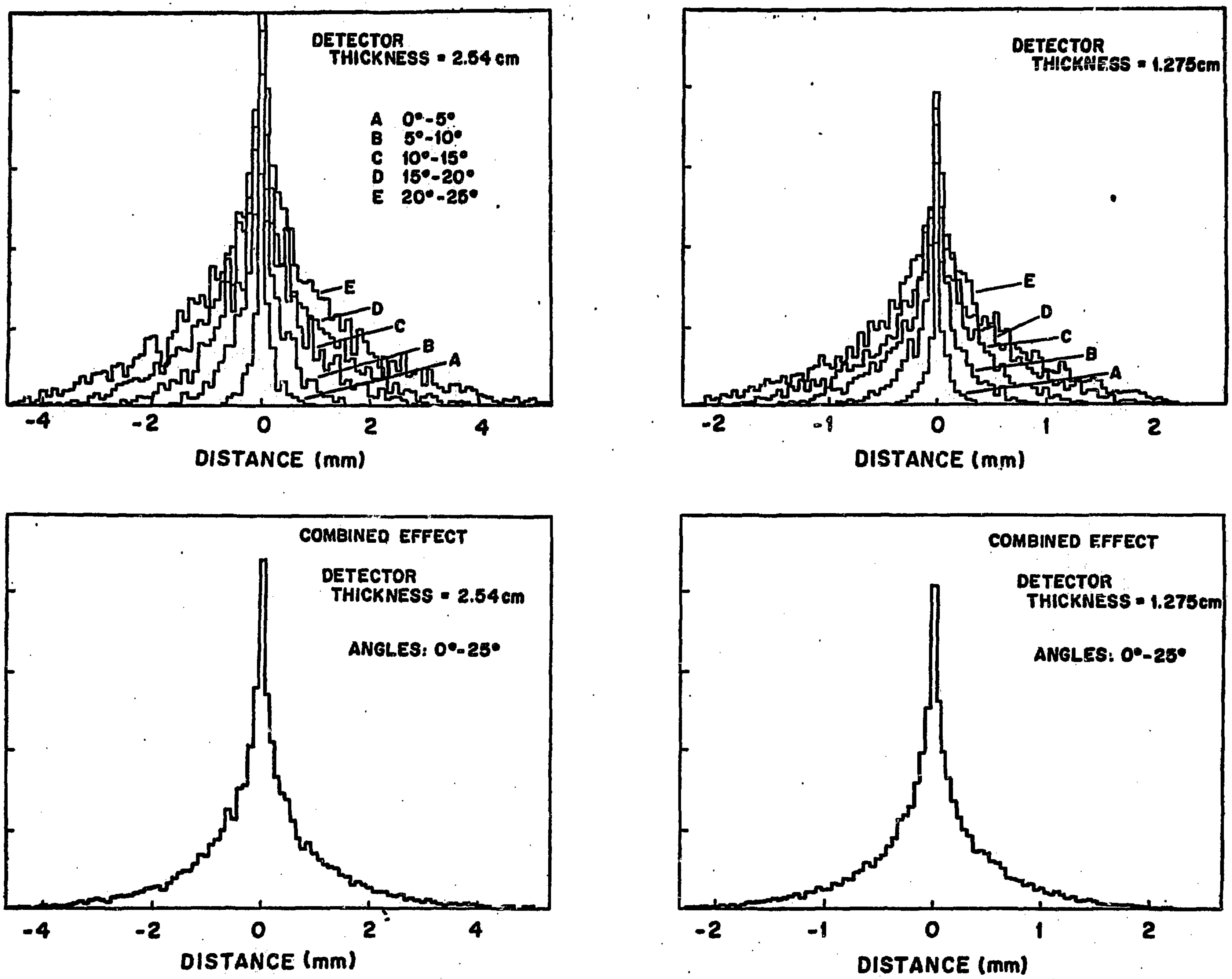

SLIDE 10

The positron-emitting nuclides chosen for investigation are ^{11}C, ^{15}O, and ^{82}Rb. These were selected since they encompass the range of positron energies of those nuclides which are considered suitable for incorporation into radiopharmaceuticals. The maximum positron energies range from .959 MeV to about 3.15 MeV with corresponding maximum linear ranges in water of 4.98 cm to 15.6 mm. These values for the maximum range might lead one to suspect that this is a significant factor in limiting the theoretical spatial resolution. This does not appear to be the case. This conclusion is indicated by the FWHM and FWTM values shown in the last two columns of this table, which were once again obtained by simulation techniques. As an example, the LSF due to the finite positron range alone is shown in the next slide for ^{11}C.

SLIDE 11

We see that this is not a Gaussian-shaped curve, but is rather peaked. This component was investigated by similar computational techniques. In this instance, positrons rather than photons were emitted isotropically from a point source at random. These were followed through a tissue equivalent medium in a probabilistic sense to the site of annihilation. The distance which the emitted positron would travel was selected at random according to an exponential probability distribution and an attenuation coefficient appropriate to the maximum positron energy. From this point, the

EFFECT OF POSITRON RANGE ON COINCIDENT RESPONSE

Radionuclide	Maximum Energy	Maximum Linear Range	FWHM	FWTM
^{11}C	.959 MeV	4.98 mm	.17 mm	1.05 mm
^{15}O	1.72 MeV	8.22 mm	.35 mm	2.08 mm
^{82}Rb	3.15 MeV	15.6 mm	.71 mm	4.20 mm

EFFECT OF POSITRON RANGE ON COINCIDENT RESPONSE FUNCTION

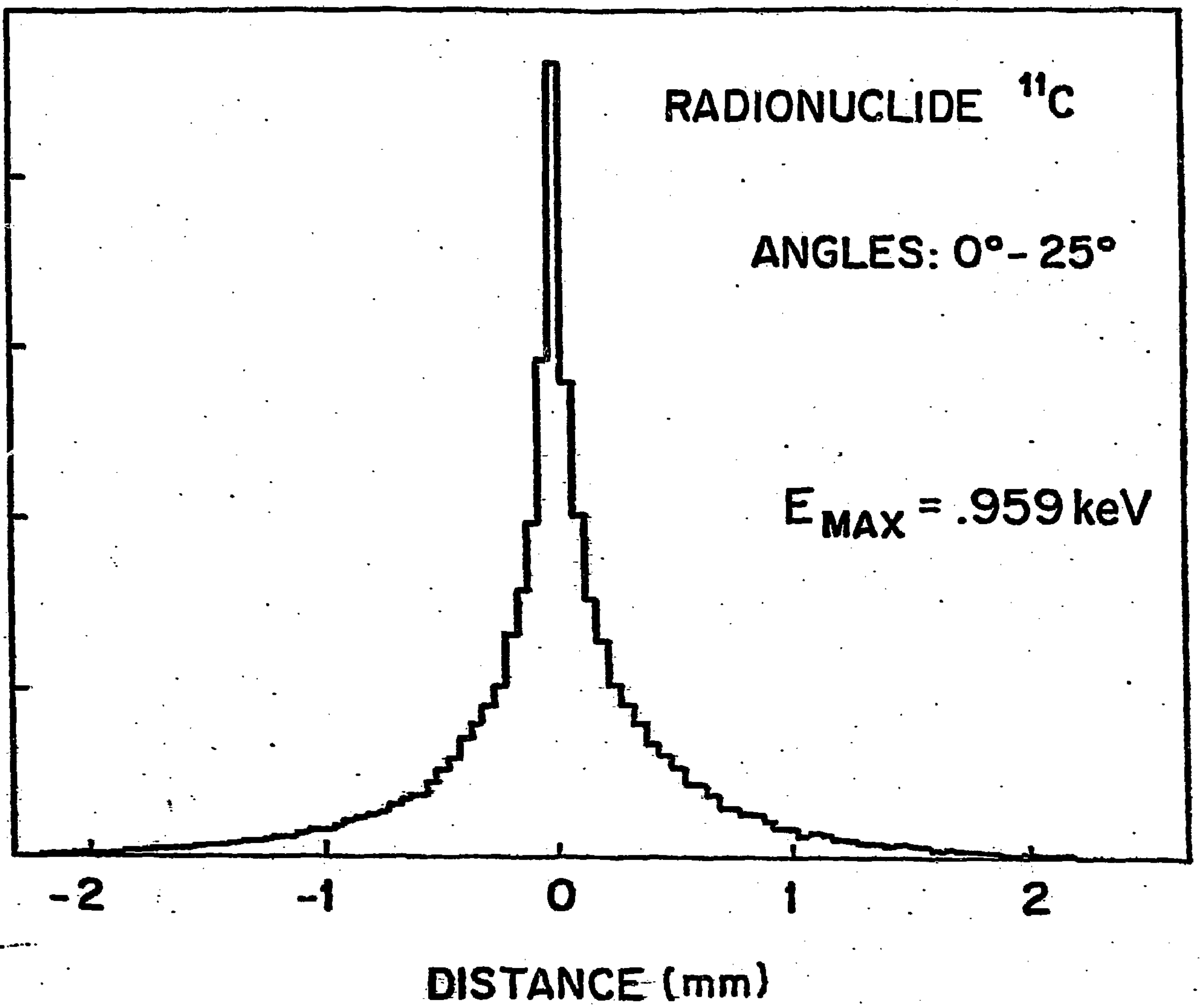

annihilation photons were emitted isotropically. This yields a spherically symmetric distribution of annihilation sites about the source. The back-projected image of this volume distribution of photon sources represents the response function due to the positron range. This will depend to some extent on the size and separation of the detectors, and in these examples they were assumed to subtend a 25° cone.

The final factor to be considered is the angular deviation of the annihilation photons from 180°. As a positron traverses a medium, it thermalizes or loses its momentum before it finally annihilates with an electron.

At the time of annihilation there still remains, however, a residual momentum associated with the positron-electron pair. This residual motion in the center-of-mass results in an angular distribution of the annihilation photons about 180°. The shape of this distribution is not, however, Gaussian. An estimate of this component was made using the experimental data of Colombino to which an empirical density function was fitted. This effect is somewhat ambiguous since this distribution is affected by the physical and chemical state of the medium, the temperature, and to some extent, the beta$^+$-decay energy of the radionuclide.

A result of this simulation is shown in the next slide.

<u>SLIDE 12</u>

This was achieved in the following manner: We begin with the isotropic emission of the first photon of the pair. An

EFFECT OF ANGULAR DEVIATION BETWEEN ANNIHILATION PHOTONS ON COINCIDENT RESPONSE FUNCTION

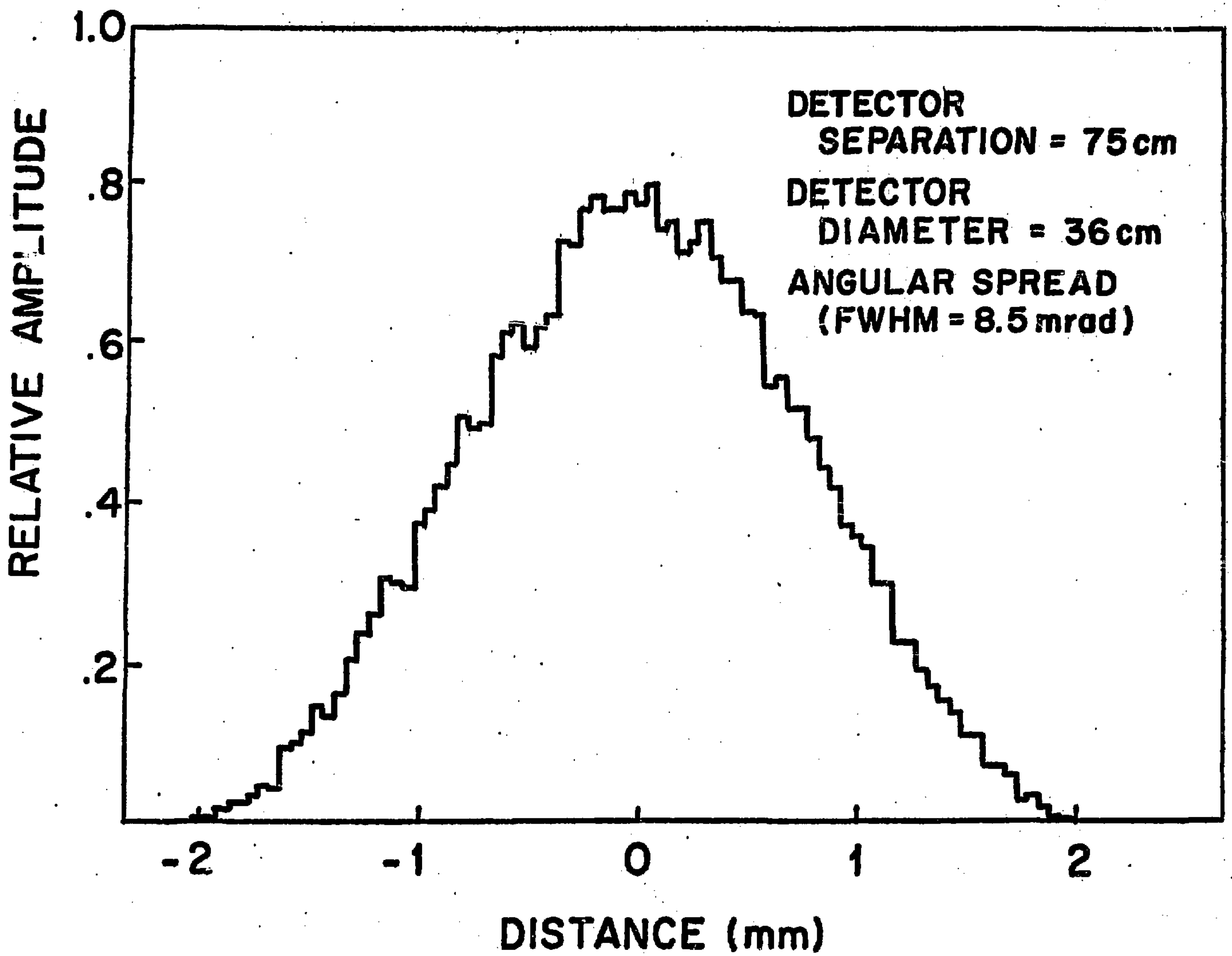

angular deviation was then selected from the empirical density function. These deviations were added to the direction cosines of the anti-parallel ray. The intercepts of these paths were computed in detector planes assumed to be 75 cm apart. The ray joining these end points was back-projected through the source plane and yields the curve shown. This produces an approximately Gaussian response with a FWHM of 1.8 mm. We have indicated how Monte Carlo techniques can be used to investigate the effects of these various factors on system resolution independently. The combined effect is, however, difficult to estimate from the individual responses because of the differences in functional form, and the coupled relationships when all are present simultaneously. An example of the net effect is shown in the last slide.

SLIDE 13

In this case, an intrinsic resolution of 7.7 mm has been assumed for a 2.54 cm thick detector, that angles up to 25° are accepted, and the source is ^{82}Rb. These parameters are of interest to our group because they are relevant to the positron camera which we have been developing in collaboration with Searle, which uses two LFOV scintillation cameras with 1"-thick crystals. The net effect is a LSF which is essentially Gaussian with a theoretical FWHM of 7.4 mm.

In conclusion, we have developed a relatively straightforward simulation approach which allows one to investigate the various

NET EFFECT ON RESOLUTION OF A POSITION CAMERA

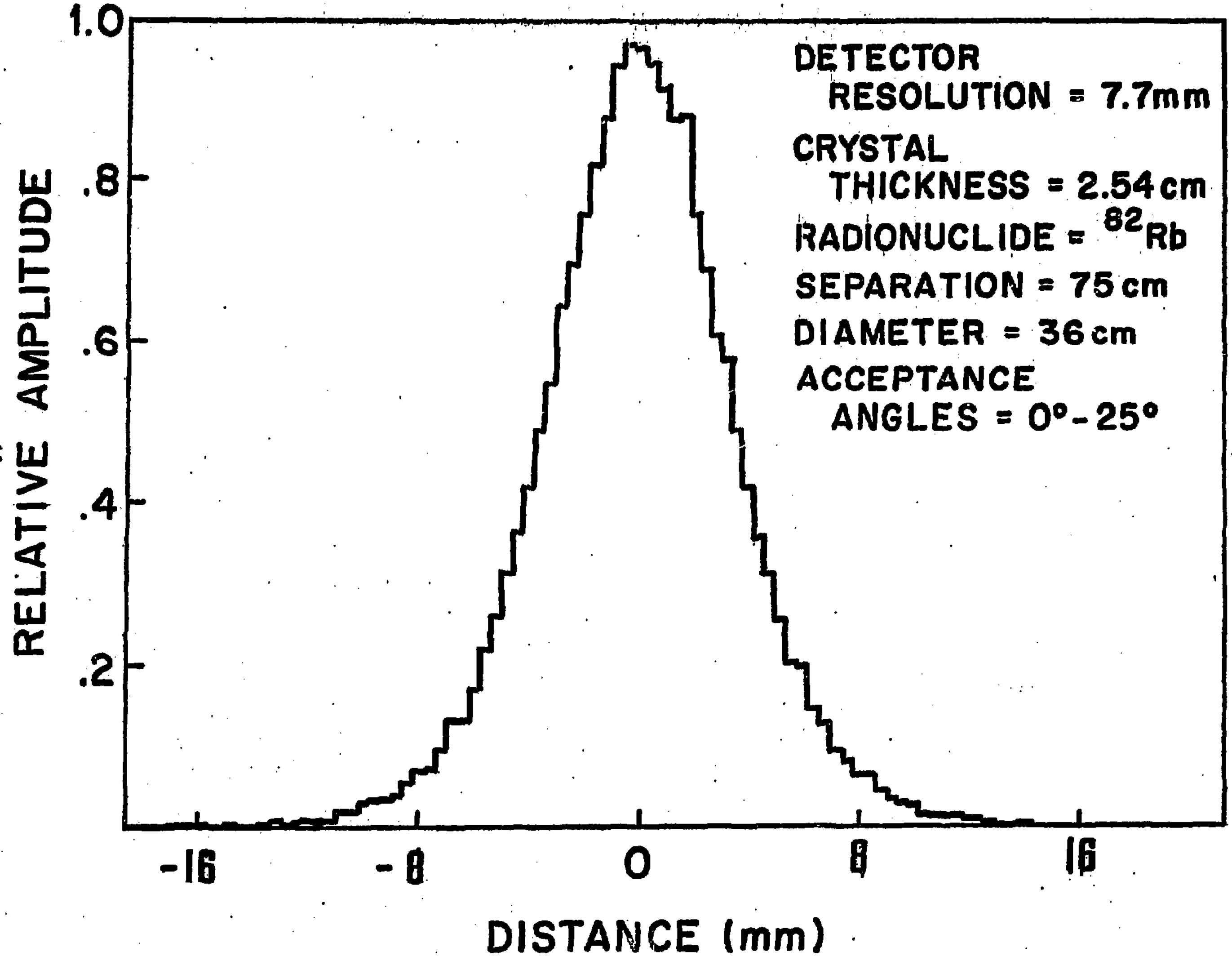

SLIDE 13

components which contribute to resolution degradation in positron cameras, and to assess their relative importance in the future design of higher resolution systems.